

## Design and modeling of an exoskeleton torque sensor

**Paweł Herbin**

West Pomeranian University of Technology Szczecin  
Faculty of Mechanical Engineering and Mechatronics  
19 Piastów Ave., 70-310 Szczecin, Poland  
e-mail: Pawel.Herbin@zut.edu.pl

**Key words:** exoskeleton, torque sensor, FEM analysis, closed loop cable conduit system, strain gauge, wearable robots

### Abstract

Controlling the upper limb with force feedback requires the continuous measurement of multiple values, so it is necessary to use a specific measuring system. The position of the joints and the torque produced by the drives are the basic feedbacks necessary for control. Measurement of the joint positions does not cause complications, while measurement of the driving torque is much more complex. This article describes the methods of implementing an exoskeleton drive system through a closed loop conduit system based on Bowden cables, and the integration of a torque sensor within the wheel of the exoskeleton. The integration of the sensor within a mechanical part of the construction of the exoskeleton is the main advantage of the developed sensor because it does not affect the dynamics of the exoskeleton. This article presents the process of designing, calibrating and validating the proposed link wheel torque sensor.

### Introduction

Exoskeletons are a special group of robots called wearable robots. Their main functions are, among others, limb support, device control or rehabilitation. Moreover, exoskeletons are equipped with a number of sensors (Huo et al., 2016) which are necessary to transmit information relevant to the control of such devices. Control of an exoskeleton's motion requires measurement of the joints' angular positions, while force feedback requires knowledge of the moments generated by the exoskeleton's drives; thus, continuous measurement of the torque generated by the drives during operation of the device is one of the most important tasks to be performed. The ExoArm 7-DOF upper-arm exoskeleton, shown in Figure 1, has seven degrees of freedom (DOF) and ensures full mobility of the human hand (Herbin & Pajor, 2017).

The exoskeleton drives are located on the external stand. Transmission of the force generated by the drives to the exoskeleton is realized through

a closed-loop cable conduit system. This system enables measurement of the driving torque by measuring the forces generated by the drives. By measuring the driving torque with a sensor that is located directly on the axis of the exoskeleton, losses caused

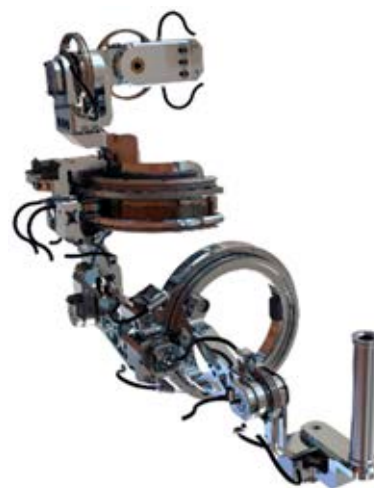


Figure. 1. The ExoArm 7-DOF upper-arm exoskeleton

by tension transmission are avoided. Examples of torque and force sensor structures are extensively documented (Yuan et al., 2014; Herbin, Pajor & Stateczny, 2016). Due to the deformability of the presented types of sensors, it is necessary to analyze their effects on the functionality of the ExoArm 7-DOF as a whole. Methods of component importance and reliability analysis have been discussed by Chybowski & Gawdzińska (2016a, 2016b) and Chybowski, Twardochleb & Wiśnicki (2016).

## The device drive system

The ExoArm 7-DOF drive employs Thompson direct current (DC) actuators. The maximum force of the DC linear actuators has been determined based on the dynamics model described by Pajor & Herbin (2015). The actuators are connected to the exoskeleton's joints by a closed-loop cable conduit system.

### Closed-loop cable conduit system

The closed-loop cable conduit system is constructed with Bowden cables. The main advantages of this system are the constant ratio of torque to the force generated by the linear actuator and the constant ratio of the angular displacement of the joint to the displacement of the actuator piston rod. Each

exoskeleton joint is equipped with two wrapping connectors. Figure 2 shows the cable conduit system; Figure 2a shows a drive stand, whereas Figures 2b and 2c show two types of exoskeleton joints.

The first type of joint is used in five joints of the ExoArm 7-DOF where the rotational axis is available; the second type of joint is used wherever there is a need for rotational movement around parts of the human body, i.e. shoulder interior/exterior rotation and elbow supination/pronation. This article focuses on the first type of joint (Figure 2b), which enables the measurement system to be mounted directly on the rotational axis of the joint.

### Modeling and development of the torque sensor

In order to perform torque measurement using a link wheel, a deformable structure has been developed that deforms in a controlled way at a specific location. The geometric form of the link wheel can be divided into an inner ring, an outer ring (truck) and four measuring beams. The link wheel is shown in Figure 3.

The outer ring acts as a truck for the wrapping connectors. The internal ring is used to transfer torque to the ExoArm 7-DOF joint. The gauge beams are bent during loading in a direction corresponding to the torque applied to the joint. Due to the symmetrical

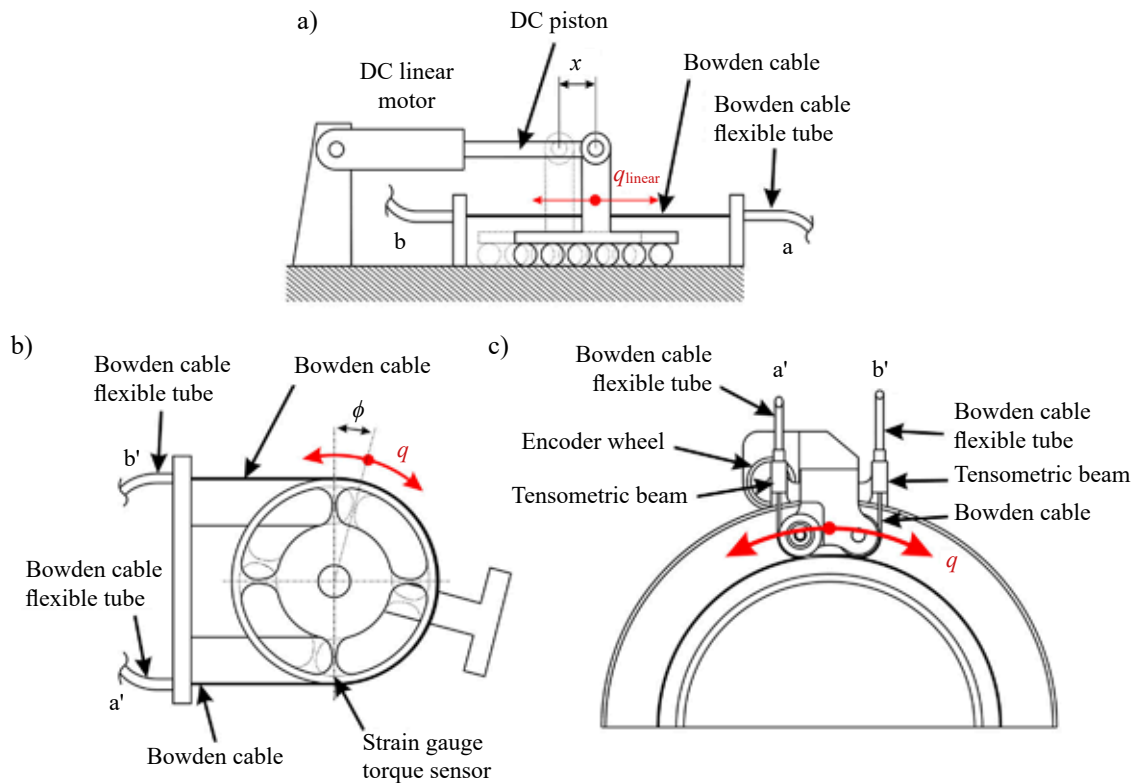


Figure 2. Schematic of two joint constructions: a) linear motor stand; b) first type of joint c) second type of joint

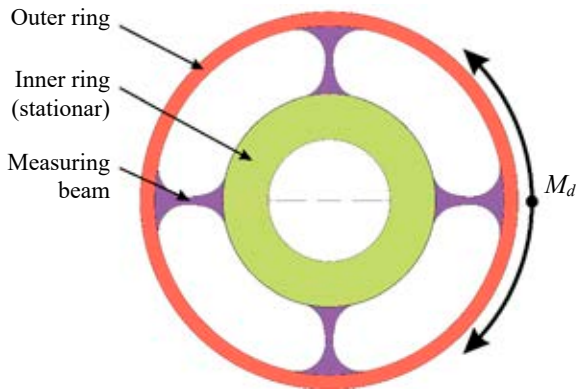


Figure 3. Schematic of the measurement link wheel

construction of this link wheel and the rigid outer ring, the deformation of each strain gauge should be identical. Strain gauges were placed on the measurement beams, configured in a full Wheatstone bridge circuit.

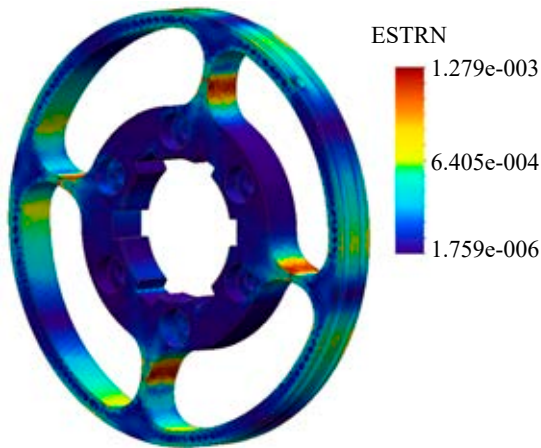


Figure 4. Deformation of a torque sensor loaded with 60 Nm

The dimensions and shape of the measurement beams were optimized in order to maximize their deformation during loading. The deformation of the sensor loaded with a torque of 60 Nm is shown in

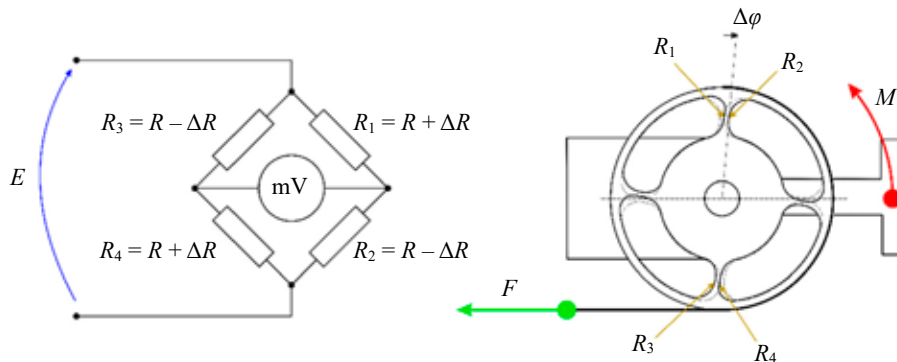


Figure 6. Schematic showing strain gauge configuration

Figure 4. During the finite element method (FEM) analysis the inner ring was fixed, while the outer ring was loaded with a force of 60 Nm.

### The prototype of torque sensor

The sensor prototype was made of 1.5026 steel alloy, which had been subjected to toughening in order to obtain a hardness of 40 HRC characterized by a Yield point,  $R_e$ , equal to 1180 MPa. To remove material between the inner and outer rings, the material was subjected to spark erosion cutting. Figure 5 shows the link wheel after machining.



Figure 5. The prototype torque sensor

In the proposed device, HBM 1-LY13-1./120 strain gauges were used which have a measurement base of 1.5 mm. Such a short measurement base is necessary because the area where the deformation reaches a maximum has a width of only 2.5 mm. Using strain gauges with such a short measuring base minimizes the possibility of improper installation of the strain gauges on the measurement beams (Chybowski, 2008). The strain gauges are configured in a full Wheatstone bridge circuit according to the Figure 6.

The strain gauges' positions on the measuring beam were determined by the FEM analysis. The arrangement of the strain gauges shown in Figure 6 is possible due to the symmetrical geometry of the link wheel.

### Testing and validation of experimental models

Strain gauges are used to measure the deformation of the measuring beam surface (Berczyński, Lachowicz & Pajor, 2001). To calibrate the sensor, the sensitivity and gain of the torque sensor were determined experimentally. The test stand used to calibrate the sensor consisted of a pneumatic actuator controlled by an air-operated pressure regulator at 8 bar (ED02 Rexroth). A dynamometer (KMM 30–1 kN Wobit) was attached to the pneumatic actuator. The measuring range of the actuator was 1 kN. For the connection of the torque sensor to the dynamometer, a 1×19 steel cable was used. The diameter of the steel cable was 2 mm. Figure 7 shows the calibration system.

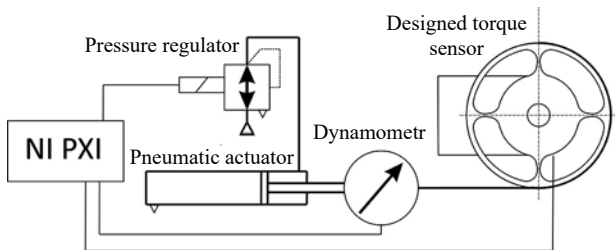


Figure 7. Scheme of the experimental stand for torque sensor calibration

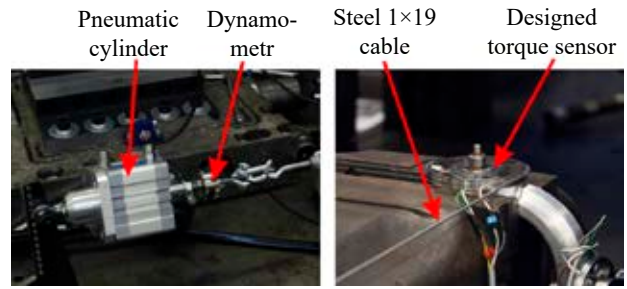


Figure 8. The test rig used for calibrating the torque sensor

During the measurements, National Instruments PXI was used with a strain gauge amplifier characterized by gain at a level of 1000. The measurement procedure was carried out in two series. The first series was responsible for tightening the wrapping connector labelled as  $a'$  in Figure 2b before the rig was modified in order to load the wrapping connector labelled as  $b'$ . This approach enabled measurements in the two directions of the developed torque sensor. The test rig is shown in Figure 8. As a result of loading the sensor with a pneumatic actuator, the dependence of the torque acting on the link wheel can be obtained from the voltage measured on the Wheatstone bridge. Results from the calibration measurements and the correlation are shown in Figure 9.

Based on the results of this research, a gain of the voltage signal has been established. This enables interpretation of the signal from the strain gauge amplifier. The obtained coefficient equals 1.5939 Nm/V. The calibrated sensor has been validated using a sinusoidal waveform with amplitude of

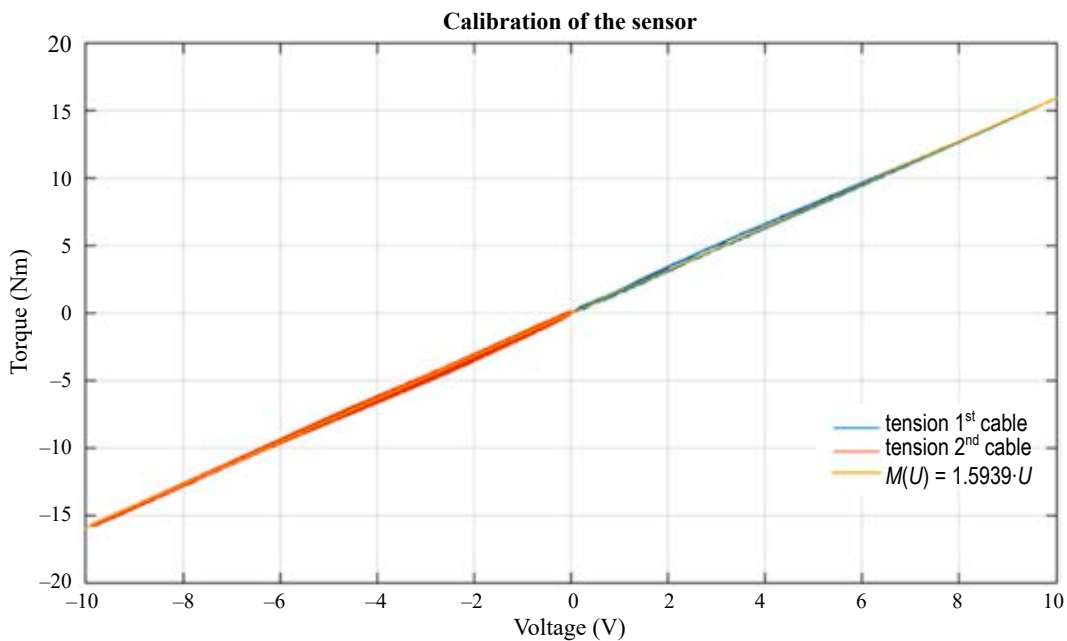


Figure 9. Results of calibration measurements and the correlation describing the dependence of torque on the measured voltage

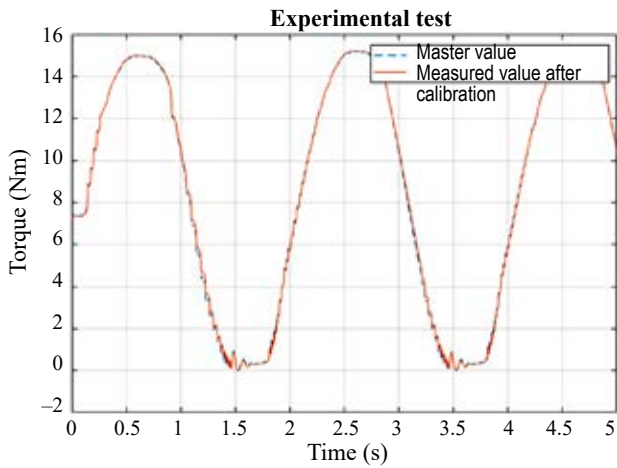


Figure 10. Validation results for torque: amplitude 15 Nm, frequency 0.5 Hz

15 Nm and frequency 0.5 Hz as shown in Figure 10. Comparisons of the reference torque signal from the dynamometer and the torque signal from the tested torque sensor for high and low loads are presented in Figures 11a and 11b respectively. It is worth noting that high torque signal compatibility was obtained during the high load. Reducing the wrapping connector tension caused differences in the indication of the design measuring system relative to the reference dynamometer. The differences between the reference torque and measured torque signals at for high and low loads are presented in Figures 12a and 12b respectively.

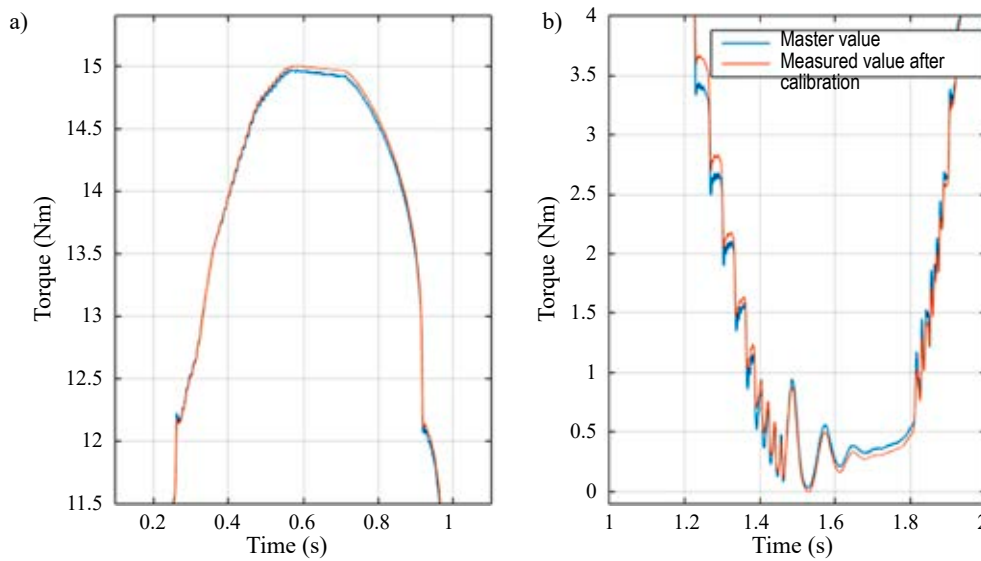


Figure 11. Comparisons of the reference torque signals from the dynamometer and measured torque signals from the tested torque sensor for: a) high load, b) low load

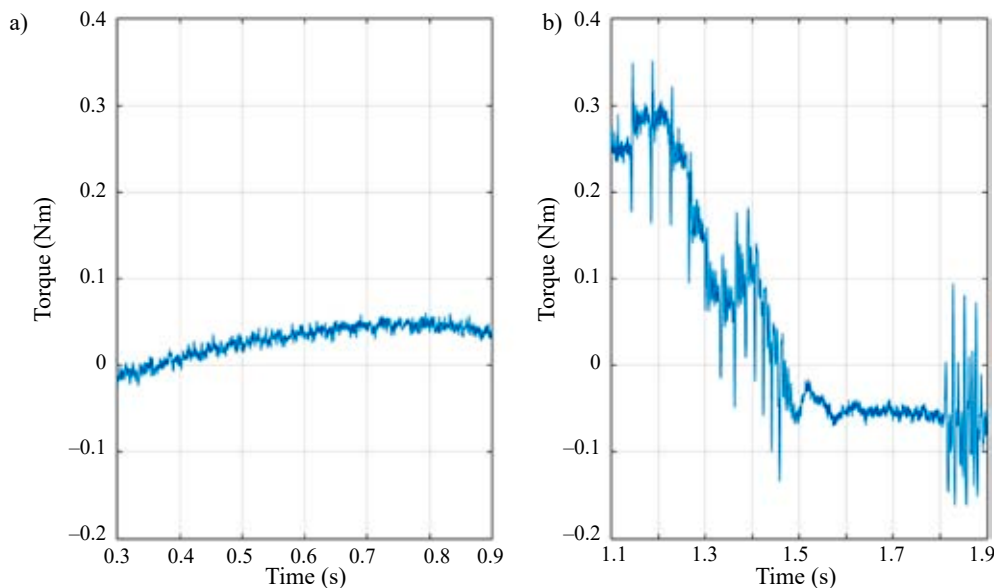


Figure 12. Differences between reference torque signal and measured torque signal using the designed torque sensor for: a) high load, b) low load



## Summary and conclusions

This article presents methods for developing and calibrating a torque sensor used in the ExoArm 7-DOF exoskeleton. The developed sensor is compact and integrated within the link wheel; thus, it does not increase the weight of the exoskeleton structure, nor does it affect the dynamics of the object. During the course of the research, it was found that the use of 1×19 steel cable lessens the accuracy of the torque sensor. This phenomenon is due to the use of too rigid a construction in the cables. Future work is planned which will exchange the wrapping connectors with cables characterized by much higher flexibility, for example 8×19+7×7, which are more flexible with only a slight decrease in the strength, assuming the same outer diameter of cable; however, the differences in the indications of the designed measuring system relative to the reference dynamometer are in the range from -0.15 to 0.34 Nm. Assuming that the joint is operating at a maximum torque of about 30 Nm during normal operation, this error equals only 1.2% of the full range of the measured torque scale.

## References

1. BERCZYŃSKI, S., LACHOWICZ, M. & PAJOR, M. (2001) An improved method of approximating frequency characteristics in the problem of modal analysis and its applications. *International Journal of Computational Methods and Experimental Measurements* X, pp. 575–584.
2. CHYBOWSKI, L. (2008) Assessment of Marine Engines Torque Load Without Using of The Torquemeter. *Journal of Polish CIMAC* 3, 1, pp. 60–68.
3. CHYBOWSKI, L. & GAWDZIŃSKA, K. (2016a) On the Present State-of-the-Art of a Component Importance Analysis for Complex Technical Systems. In: Á. Rocha et al. (eds.), *New Advances in Information Systems and Technologies, Advances in Intelligent Systems and Computing* 445, pp. 691–700. Switzerland: Springer International Publishing, doi: 10.1007/978-3-319-31307-8\_70.
4. CHYBOWSKI, L. & GAWDZIŃSKA, K. (2016b) On the Possibilities of Applying the AHP Method to a Multi-criteria Component Importance Analysis of Complex Technical Objects. In: Á. Rocha et al. (eds.), *New Advances in Information Systems and Technologies, Advances in Intelligent Systems and Computing* 445, pp. 701–710, Switzerland: Springer International Publishing, doi: 10.1007/978-3-319-31307-8\_71.
5. CHYBOWSKI, L., TWARDOCHEŁB, M. & WIŚNICKI, B. (2016) Multi-criteria Decision making in Components Importance Analysis applied to a Complex Marine System. *International Journal of Maritime Science & Technology "Our sea", "Naše more"* 63 (4), pp. 264–270, doi: 10.17818/NM/2016/4.3.
6. HERBIN, P. & PAJOR, M. (2017) *Interactive 7-DOF Motion Controller of The Operator Arm (ExoArm 7-DOF)*. In: Innovations in Intelligent Systems and Applications (INISTA), International Symposium (pp. 185–188). IEEE. doi: 10.1109/INISTA.2017.8001154
7. HERBIN, P., PAJOR, M. & STATECZNY, K. (2016) Six-axis control joystick based on tensometric beam. *Advances in Manufacturing Science and Technology* 40, 4, pp 33–41.
8. HUO, W., MOHAMMED, S., MORENO, J.C. & AMIRAT, Y. (2016) Lower limb wearable robots for assistance and rehabilitation: A state of the art. *IEEE Systems Journal* 10, 3, pp. 1068–1081.
9. PAJOR, M. & HERBIN, P. (2015) Egzoszkieleł koŃczyzny górnej-model z wykorzystaniem rzeczywistych parametrów ruchu. *Modelling in Engineering, Modelowanie Inżynierskie* 26, 57, pp. 40–46.
10. YUAN, C., YAN, R.J., WU, J., KIM, S.H., SHIN, K.S. & HAN, C.S. (2014) *Design and evaluation of a three-axis force/torque sensor for humanoid robot balance control*. In: Control, Automation and Systems (ICCAS), 14<sup>th</sup> International Conference (pp. 227–232). IEEE. doi: 10.1109/ICCAS.2014.6987991